Kim and Shin *Applied Biological Chemistry* (2022) 65:21
https://doi.org/10.1186/s13765-022-00690-1

KSABC
The Korean Society for Applied Biological Chemistry

ARTICLE Open Access

IC261 inhibits the epithelial-mesenchymal transition induced by TGF-β in A549 lung cancer cells

Sung Jim Kim and Myoung-Sook Shin*

Abstract

Despite rapid advances in cancer diagnosis and therapy, lung cancer continues to be the primary cause of cancer-related mortality. Epithelial mesenchymal transition has been implicated in drug resistance and cancer metastasis. IC261 mediates various pathophysiological processes, including inflammation and tumorigenesis. Therefore, we analyzed the involvement of IC261 in epithelial mesenchymal transition. Pretreatment with IC261 significantly inhibited the expression of transforming growth factor (TGF)-β1-induced mesenchymal cell markers, including N-cadherin (N-cad), vimentin (Vim), and β-catenin (β-cat), at the mRNA and protein levels in A549 lung cancer cells, which was confirmed using immunofluorescence staining. A migration assay revealed that IC261 treatment strongly inhibited TGF-β1-induced migration activity at 24 and 48 h. Additionally, IC261 treatment suppressed the activation of the TGF-β1 signaling pathway in A549 cells and phosphorylation of Smad2 and Smad3. Our findings demonstrate that IC261, a selective inhibitor of casein kinase 1, inhibits the TGF-β1-induced migration of A549 cells by inhibiting Smad2/3 phosphorylation and downregulating the expression of N-cad, Vim, and β-cat.

Keywords: Epithelial mesenchymal transition, IC261, Smad2, Samd3

Introduction

Metastasis means that cancer cells spread into the body and form secondary tumors. It is known that 90% of cancer patients die due to cancer metastasis [1]. The incidence and mortality of lung cancer are highest among all cancer worldwide, including in Europe, North America, and China [2, 3]. Lung cancer is more common in males than in females [2] and is typically classified into two distinct subtypes: non-small cell lung cancer (NSCLC) and small cell lung cancer, with NSCLC accounting for around 85% of lung cancer cases. Nearly 25–33% of patients with NSCLC progress to stage I or II disease and undergo surgical resection with curative intent. Nevertheless, approximately 30–40% of patients with NSCLC with negative lymph nodes and discrete lesions die from recurrent disease [4]. Nearly 80% of all lung cancer-related deaths are caused by NSCLC. In the European Union, nearly 270,000 people were expected to die from lung cancer in 2013. The survival rate of patients with lung cancer remains unchanged to this date [5]. Lung cancer remains incurable despite recent advances in diagnostic and operative techniques; however, chemotherapy can improve the efficiency of lung cancer therapy [5, 6].

The precise molecular mechanism by which cancer metastasizes remains unknown. Numerous recent investigations have established that the epithelial mesenchymal transition (EM transition transition) is a critical molecular mechanism promoting cancer metastasis [7, 8]. EM transition is a biological process in which epithelial cells undergo a series of changes in their morphology, architecture, adhesion, and motility to acquire a mesenchymal cell phenotype [9]. This process occurs during wound healing, tumor progression, and organ fibrosis. [10–12]. EM transition is typically defined by

*Correspondence: ms.shin@gachon.ac.kr
Gachon University, Seongnam 13120, Korea

the degeneration of cell–cell junctions; remodeling of the actin cytoskeleton; separation of cells; apical-basal polarity; gain of migratory and invasive properties, such as spindle-shaped and motile cells; and manifestation of mesenchymal markers, including fibronectin, N-cadherin (N-cad) and vimentin (Vim) [13]. EM transition plays an important role in embryonic development, wound healing, and cancer metastasis [14–18]. Mesenchymal cells move away from the original tumor and invade the blood vasculature during EM transition. Because EM transition is a dynamic and flexible process, mesenchymal cells undergo a reverse process known as mesenchymal epithelial transition, in which they revert to their original epithelial phenotype and proliferate at distant metastatic tissues via different mechanisms, such as via altered stromal interactions [9, 14, 15]. Additionally, many factors induce EM transition in cancer cells, such as oxidative and hypoxic stresses. Considering the complex mechanisms involved in EM transition, determining its mechanism is key to developing new therapeutic approaches for cancer treatment and preventing cancer metastasis [9, 19–21].

IC261 is a well-characterized inhibitor of protein kinases, casein kinase 1δ (CK1δ) and CK1ε [22]. Furthermore, it is involved in DNA replication, induces p53-mediated arrest of cells, and affects cell cycle progression [22]. CK1 inhibition by IC261 was shown to influence pancreatic cancer and colon cancer cell growth and apoptosis sensitivity as well as reduce tumors in vivo [23, 24]. However, studies on inhibitory effects on EM transition targeting lung cancer using IC261 have not been reported. The aim of this study was to establish IC261's potential function and molecular mechanisms of action as an EM transition inhibitor. Therefore, we synthesized IC261 and examined the effect of IC261 on EM transition and explored their possible mechanisms using A549 lung cancer cells. The results of our study show that IC261 was found to significantly decrease the expression of TGF-β-induced mesenchymal cell markers as well as the capacity of cells to migrate via Smad2/3 phosphorylation in A549 cells.

Materials and methods

Synthesis of IC261

The reaction mixture consisting of indolin-2-one (39.0 mg, 0.3 mmol) and 2,4,6-trimethoxybenzaldehyde (58.0 mg, 0.3 mmol) in methanol (1 mL) was treated with piperidine (30 µL, 0.36 mmol) in a sealed tube. The mixture was allowed to react overnight at 100 °C; the resultant mixture was extracted with ethyl acetate (20 mL, thrice) and H_2O (20 mL, thrice). The extracted organic layer was dried over anhydrous Na_2SO_4, and the solvent was concentrated by evaporation. Column chromatography on silica gel (ethyl acetate/hexane = 3:2) was performed to purify the crude mixture to yield IC261, which was dried to its solid form. ^{1}H-NMR (400 MHz, $CDCl_3$); δ 8.42 ppm (s, NH, 1H), 7.76 ppm (s, 1H), 7.13 ppm (td, J = 6.12 Hz, 1.0 Hz, 1H), 6.96 ppm (dd, J = 6.44 Hz, 1.04 Hz, 1H), 6.88 ppm-6.83 ppm (m, 2H), 6.20 ppm (s, 2H), 3.89 ppm (s, 3H), and 3.77 ppm (s, 6H). ^{13}C-NMR ($CDCl_3$) 170.59, 163.1, 159.8, 140.9, 129.0, 128.5, 127.6, 124.6, 123.6, 121.5, 109.4, 106.2, 90.5, 55.7, 55.6 ppm. MS (ESI) calculated for $C_{18}H_{18}NO_4$ $[M+H]^+$ *m/z* 312.12, observed *m/z* 312.1 (Additional file 1: Figure S1).

Antibodies and reagents

Primary antibodies against N-cad (D4R1H), E-cad (24E10), Vim (D21H3), β-cat (D10A8), GAPDH, and Smad2/3 were supplied by Cell Signaling Technology (Danvers, MA, USA). Phosphospecific antibodies against Smad2 and Smad3 were also sourced from Cell Signaling Technology. RPMI 1640 medium and Dulbecco's phosphate buffered saline (DPBS) were from Corning, Inc. (Corning, NY, USA). TGF-β1 was supplied by Cell Signaling Technology. SlowFade™ Gold antifade reagent with DAPI, Alexa Fluor™ 488 goat anti-rabbit IgG (H + L), and Texas Red™-X goat anti-rabbit IgG (H + L) were from Invitrogen (Carlsbad, CA, USA). The 8-well glass-chamber cover slide was obtained from SPL (Seoul, Korea). Tris-buffered saline containing Tween 20 was obtained from T&I (Chuncheon, Korea). The human lung cancer cell line (A549) was obtained from the Korea Cell Line Bank (Seoul, Korea) and cultured in completed culture medium (RPMI 1640 containing 10% fetal bovine serum and 1% penicillin–streptomycin) in a conventional cell culture incubator (37 °C incubator 5% CO_2).

A549 cell viability assay

The 96-well flat-bottomed microplates were seeded with A549 cells (5.0×10^4 cells/well). IC261 was diluted in RPMI 1640 (final concentrations: 50 and 80 µM). A549 cells were incubated with IC261 for 48 h; the cells were then incubated with EZ-Cytox solution. Cell viability was calculated by measuring the absorbance at 450 nm with a 96-well flat-bottomed plate reader. The percentage of viable cells was determined by comparing the absorbance in the experimental wells with that in the control well.

Immunoblotting

The 96-well flat-bottomed microplates were seeded with A549 cells (3.0×10^5 cells/well) for 18 h and then incubated for 6 h in serum-free culture medium (SFCM). The cells were treated with diluted IC261 (final concentrations: 50 and 75 µM) for 4 h and then stimulated with TGF-β1 for 42 h (for E-cad, N-cad, Vim, and β-cat protein

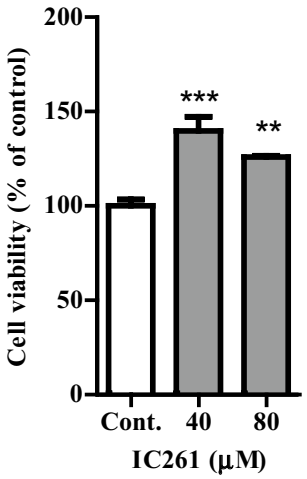

Fig. 1 Effect of IC261 on the viability of A549 cells. A549 cells (5.0×10^4 cells/well, 96-well plate) were incubated with 40 and 80 μM IC261 for 48 h, and cell cytotoxicity was evaluated using an EZ-Cytox solution. The data are presented as the mean ± SD (n = 3). $^{**}P < 0.001$ and $^{***}P < 0.0001$ compared with the control group

expression) or 30 min (for phspho-Smad2 and phosphor-Smad3 expression). The cells were rinsed with cold Dulbecco's phosphate buffered saline (Welgene, South Korea) and lysed using cold radioimmunoprecipitation assay buffer (T&I) containing a protease inhibitor (Sigma, St. Louis, MO, USA), a phosphatase inhibitor cocktail, and dithiothreitol (Merck, Darmstadt, Germany). Proteins were extracted from the cell lysates by centrifugation at 16,000 rpm for 20 min at 4 °C; the protein concentration in each sample was standardized by normalization. Sodium dodecyl sulfate–polyacrylamide gel electrophoresis was performed to separate the proteins in 10–12% polyacrylamide gels (Bio-Rad, Hercules, CA, USA), which were then transferred to a hydrophobic polyvinylidene difluoride western blotting membrane (Millipore, Billerica, MA, USA). The membrane was blocked overnight at 4 °C in 3% skim milk in Tris-buffered saline containing Tween 20 (washing buffer). After 6 h of primary antibody staining, the membrane was washed washing buffer and probed with anti-rabbit IgG secondary antibodies conjugated with horseradish peroxidase. Enhanced chemiluminescence SuperSignal West FEM transition transitiono reagent (ECL, Pierce, Rockford, IL, USA) and a Fusion Solo Chemiluminescence System (Vilber, Lourmat, Paris, France) were used to identify the protein bands.

Quantitative reverse transcription polymerase chain reaction

The 96-well flat-bottomed microplates were seeded with A549 cells (3.0×10^5 cells/well) for overnight culture; the cells were then incubated for 6 h in SFCM. IC261 (final concentrations: 50 and 75 μM) was added to the cells and cultured for 4 h, followed by stimulation with TGF-β1 for 24 h. Total RNA was extracted using an RNeasy mini kit (Qiagen, Hilden, Germany) in accordance with the supplier's protocol. Total RNA (2 μg) was reverse-transcribed into cDNA using AccuPower RT PreMix (Bioneer, Daejeon, Korea) in accordance with the manufacturer's instructions. Quantitative reverse transcription polymerase chain reaction was conducted using SYBR Green Master Mix (Applied Biosystems, Foster City, CA, USA) utilizing the following sense and anti-sense primers: Vim: 5′-GAGGATACCACTCCCAACAG-3′ and 5′-AAGTGCATCATCGTTGTTCA-3′; β-cat: 5′-GCC TCTTCTCATTCCTGCTTG-3′ and 5′-CTGATGAGA GGGAGGCCATT-3′; N-cad: 5′-GCCTCTTCTCATTCC TGCTTG-3′ and 5′-CTGATGAGAGGGAGGCCATT-3′; β-tubulin (used as a normalization control gene). The reaction was performed using a Quantstudio 3 real-time PCR system (Applied Biosystems) as follows: 40 cycles of 95 °C for 15 s and 58 °C for 1 min for all primer pairs. Relative mRNA expression was quantified using the ΔΔCt method.

Immunofluorescence analysis

A549 cells were seeded onto an 8-welled glass chambered slide (3.0×10^4 cells/well) and incubated overnight. After 4 h of treatment with the appropriate concentration of IC261, the cells were stimulated with TGF-β1 for 42 h. The cells were rinsed five times with DPBS, fixed for 15 min in 4% paraformaldehyde, and washed three times with DPBS. The cells were blocked with 5% normal goat serum in PBS for 2 h. The cells were incubated with antibodies against Vim and N-cad overnight. The cells were rinsed three times with DPBS for 1 h with the suitable secondary antibody, Alexa Fluor 488-conjugated goat anti-rabbit (for Vim) or Texas Red-conjugated goat anti-rabbit antibody (for N-cad). The cells were

(See figure on next page.)

Fig. 2 IC261 inhibits epithelial mesenchymal transition marker protein expression stimulated by TGF-β1 in A549 cells. A 6-well plate containing serum-free culture medium was seeded with A549 cells and incubated for 6 h. After 4 h of treatment with IC261 (50 and 75 μM), the cells were stimulated with TGF-β1 for 48 h. Specific antibodies were used for immunoblotting of the cell lysates. **A** Expression of N-cad, Vim, β-cat, and E-cad. **B** Protein expression level was determined using ImageJ software and normalized against the expression of GAPDH. The data are expressed as the mean ± SD (n = 3). $^{\#}P < 0.0001$ in comparison to the control and $^{***}P < 0.0001$ compared with the TGF-β1 group

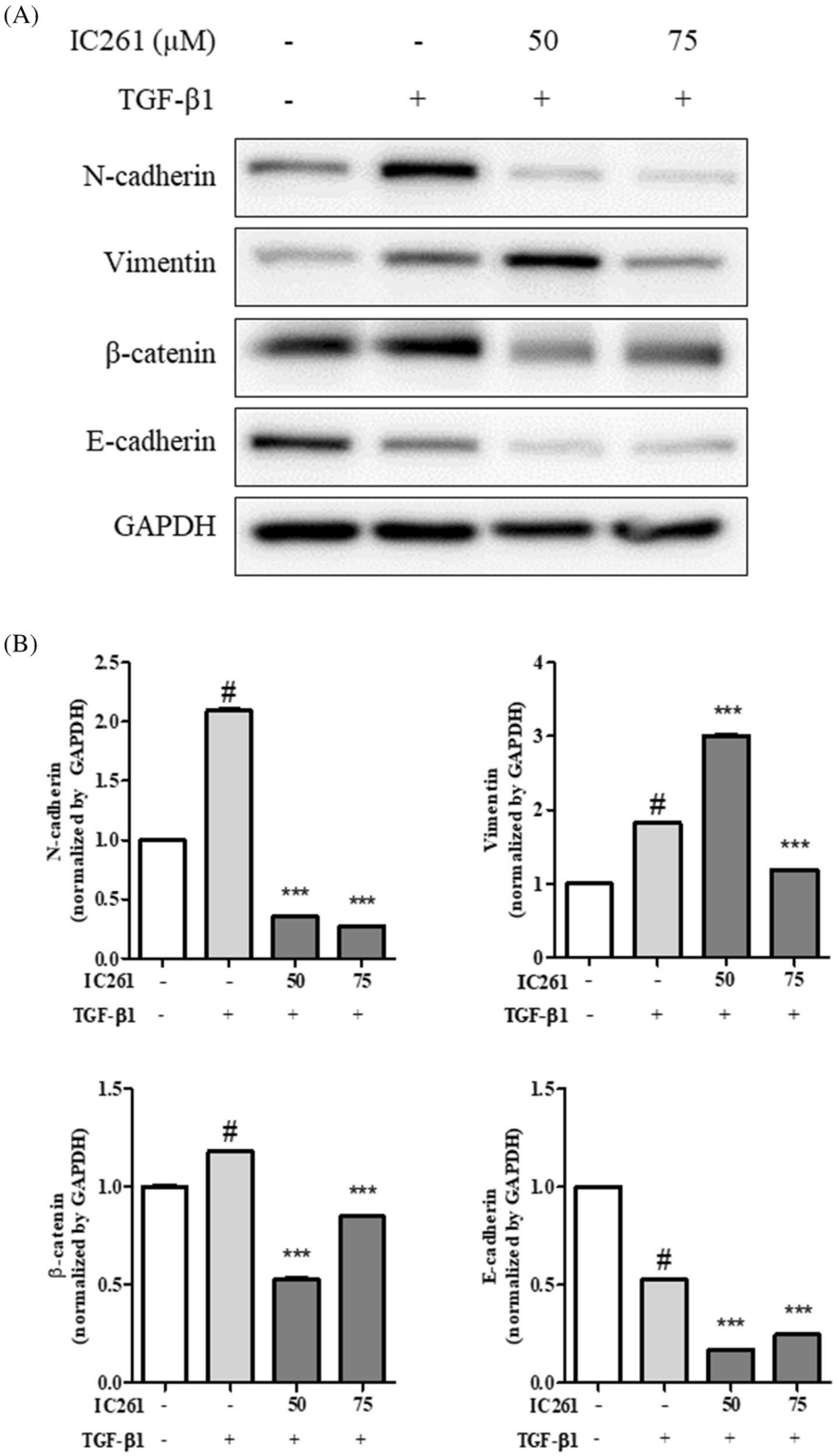

Fig. 2 (See legend on previous page.)

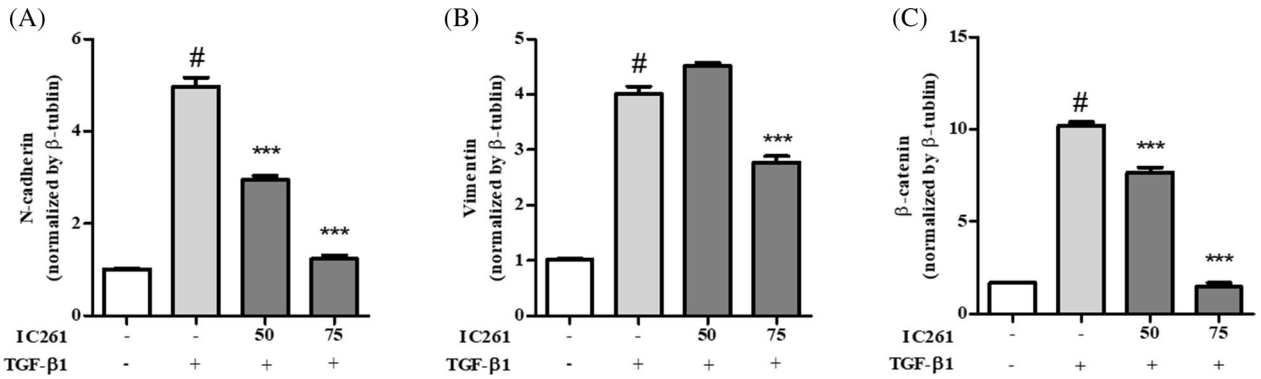

Fig. 3 Effects of IC261 on mRNA expression in TGF-β1-induced epithelial mesenchymal transition in A549 cells. A 6-well plate containing serum-free culture medium was seeded with A549 cells and incubated for 6 h. After 4 h of treatment with IC261 (50 and 75 M), the cells were stimulated with TGF-β1 for 24 h. The mRNA expression of N-cad, Vim, and β-cat was analyzed using quantitative reverse transcription polymerase chain reaction (A–D). All data are shown as the mean ± SD (n = 3). $^{\#}P < 0.0001$, compared with the control, and $^{***}P < 0.0001$ compared with the TGF-β1 group

counterstained with DAPI for 10 min at ambient temperature. Fluorescence levels were measured and evaluated using an LSM700 confocal microscope and ZED 2.3 software (Carl Zeiss, Oberkochen, Germany).

Wound healing assay

A549 cells (5.0×10^5 cells/well) were seeded into a 6-well plate and incubated overnight. IC261 (final concentrations: 50 and 75 μM) was added to the cells for another 6 h of culture, followed by stimulation with TGF-β1 for 48 h. The cells were scratched with a 200 μL tip to generate a wound, and the culture plates were rinsed with warm PBS to remove detached cells. Three photomicrographs of each scratch were obtained at the time of wound creation, and at 0, 24, and 48 h. The relative wound width was calculated as the ratio of the width of the remaining wound at each time point to the corresponding width at 0 h using ImageJ software (NIH, Bethesda, MD, USA). Three wounds and images were sampled for each treatment, and experiments were carried out in triplicate.

Statistical analysis

The mean ± standard deviation (SD) of duplicate or triplicate experiments is reported. GraphPad Prism 8 software (GraphPad, Inc., San Diego, CA, USA) was used for statistical analysis. The results were statistically analyzed with Mann–Whitney test, and differences with $P < 0.05$, $P < 0.005$, and $P < 0.0001$ were considered as significant.

Results

IC261 affects the viability of A549 cells

The cytotoxicity of IC261 towards A549 cells was assessed. Treatment of A549 cells with IC261 for 48 h did not induce cytotoxicity at 40 and 80 μM (Fig. 1). Since the cytotoxicity by the IC261 can induce EM transition inhibition, concentrations without cytotoxicity were selected. Therefore, a concentration of below 80 μM was applied in subsequent experiments.

IC261 inhibits TGF-β1-induced EM transition in A549 cells

Cancer cells undergoing EM transition display lower levels of epithelial cells markers, such as E-cad, claudin-1, and occluding, and higher levels of mesenchymal cell markers, such as N-cad, Vim, β-cat, and fibronectin [9]. To determine whether IC261 inhibits TGF-β1-induced EM transition in A549 cells, we analyzed the protein levels of EM transition markers. As shown in Fig. 2, TGF-β1 upregulated the expression of N-cad, Vim, and β-cat and downregulated that of E-cad. Although IC261 treatment effectively suppressed the TGF-β1-induced expression of N-cad, Vim, and β-cat in A549 cells, that of E-cad remained downregulated (Fig. 2A). Figure 2B shows the graph used to quantify the immunoblotting results shown in Fig. 2A. Taken together, our findings suggest that IC261 inhibits EM transition in A549 cells.

Effects of IC261 on N-cad, Vim, β-cat, and E-cad mRNA expression in A549 cells with TGF-β1-induced EM transition transition

Because IC261 significantly inhibited TGF-β1-induced mesenchymal markers in A549 cells at the protein level, we evaluated whether IC261 inhibits the mRNA expression of N-cad, Vim, and β-cat. As shown in Fig. 3, after TGF-β1 treatment for 24 h, the mRNA expression of N-cad, Vim, and β-cat increased compared with that in the control. In

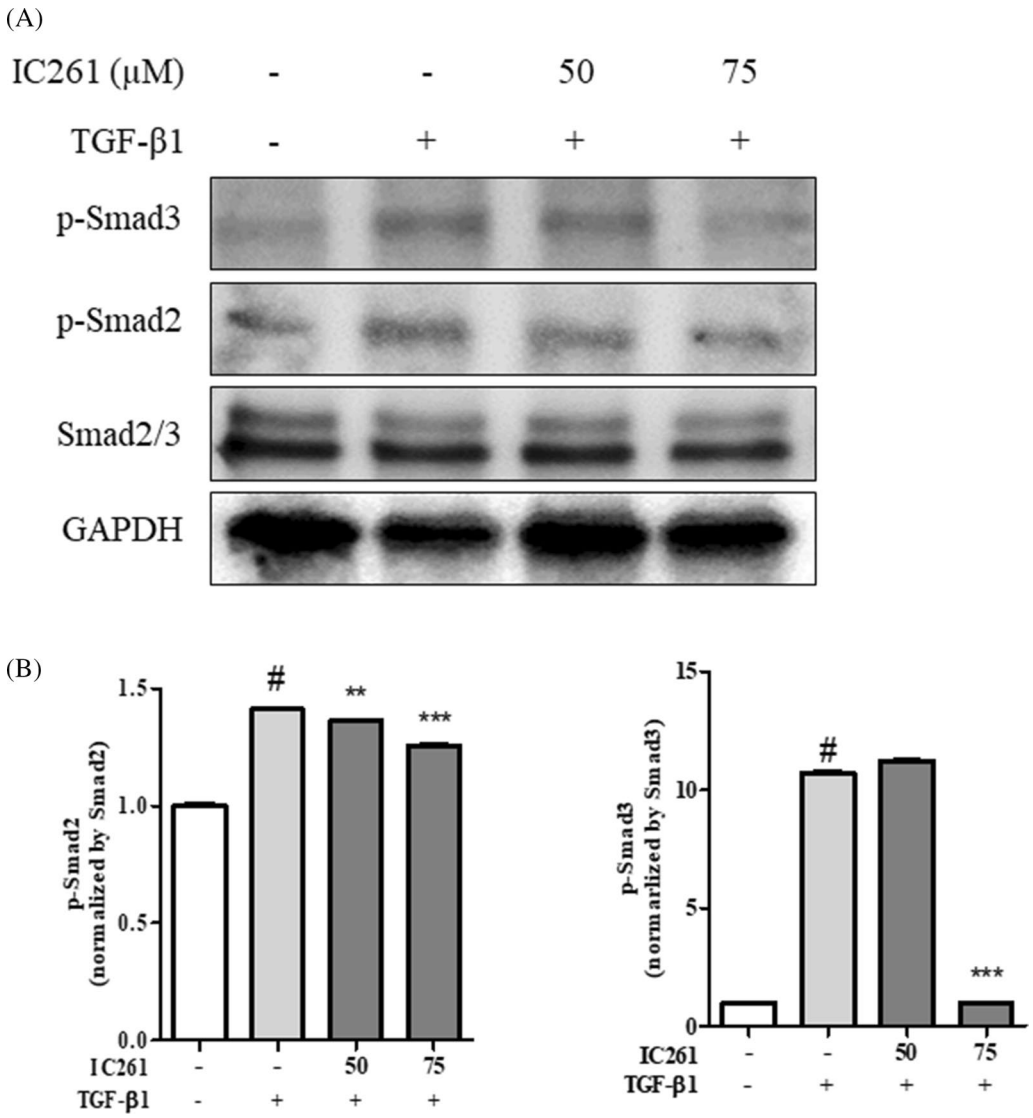

Fig. 4 Effects of IC261 on TGF-β1-induced phosphorylation of Smad2/3 in A549 cells. A 6-well plate containing serum-free culture medium was seeded with A549 cells and incubated for 6 h. The cells were treated with IC261 (50 and 75 μM) for 4 h, and then stimulated with TGF-β1 for 30 min. The expression levels of phospho-Smad2, phospho-Smad3, Smad2 and Smad3, and GAPDH were analyzed using immunoblotting (**A**). Protein expression was quantified using ImageJ software and normalized against Smad2/3 expression. The data are presented as the mean ± SD (n = 3). $^{\#}P < 0.0001$ compared with the control, and $^{***}P < 0.0001$ and $^{**}P < 0.001$ compared with the TGF-β1 group

contrast, pretreatment with IC261 decreased the TGF-β1-stimulated mRNA expression of N-cad, Vim, and β-cat (Fig. 3). These results suggest that TGF-β1 regulates the mRNA expression of N-cad, Vim, and β-cat, which was inhibited by IC261 treatment.

Effects of IC261 on TGF-β1-stimulated phosphorylation of Smad2 and Smad3 in A549 cells

The phosphorylation of Smad2 and Smad3 plays a central role in the TGF-β1 signaling pathway. TGF-β1 stimulation results in the formation of a heterogeneous complex

(See figure on next page.)

Fig. 5 Effects of IC261 on TGF-β1-induced expression of epithelial mesenchymal transition markers. A549 cells were seeded into a coverslip and incubated with serum-free culture medium for 6 h. The cells were treated with IC261 (50 and 75 μM), and then stimulated with TGF-β1 for 42 h. The cells were fixed and stained with antibodies against Vim (upper) and N-cad (lower), followed by incubation with fluorescent dye-tagged secondary antibodies. The nuclei were stained using DAPI. Vim and N-cad were visualized using a confocal microscope

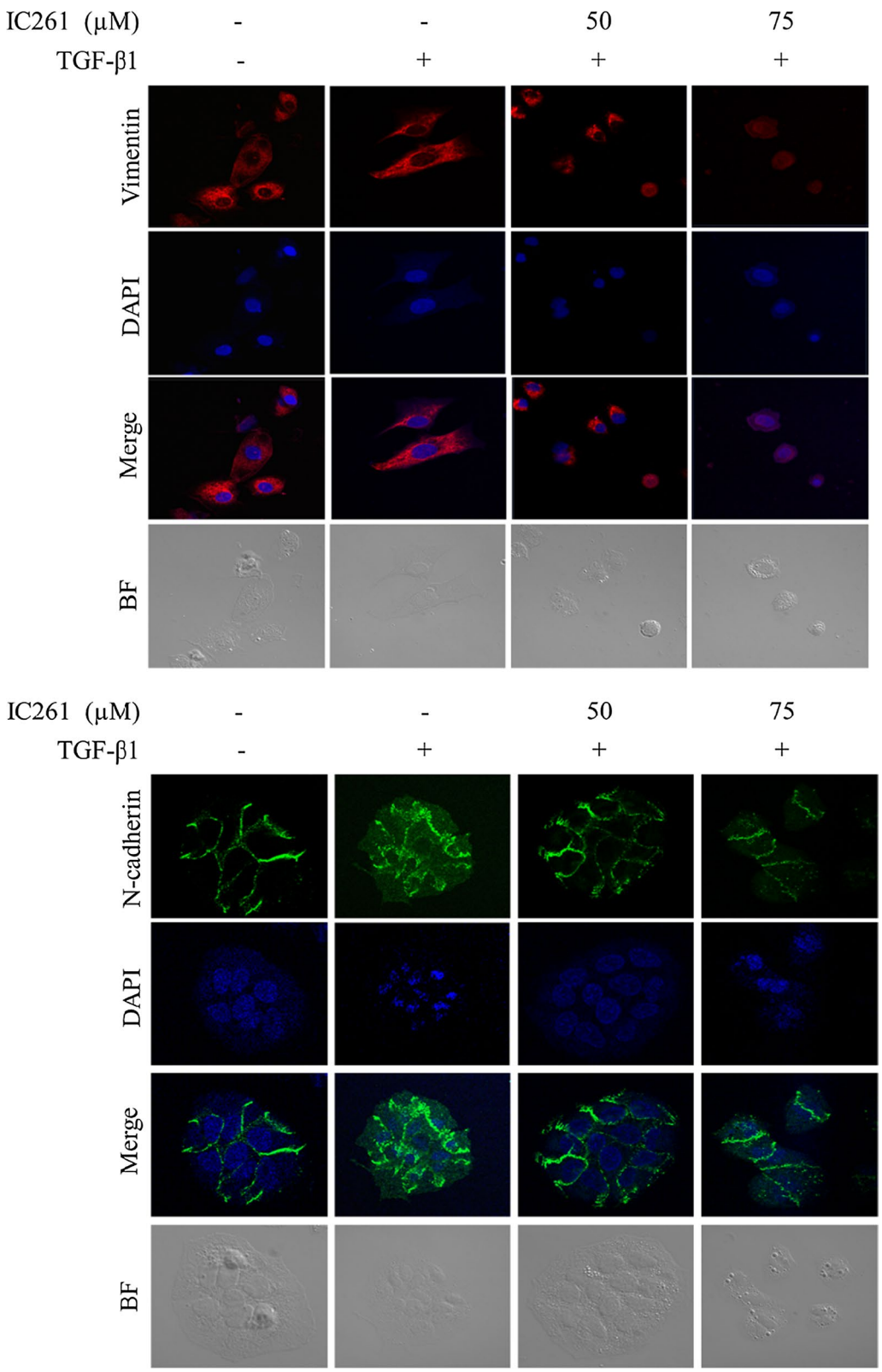

Fig. 5 (See legend on previous page.)

of Smad2 and Smad3 with the mediator Smad4 (co-Smad). The Smad2/3/4 complex translocate to the nucleus, where it binds to transcription factors, co-repressors, and co-activators to regulate EM transition-related genes [25, 27]. To determine whether IC261 inhibits TGF-β1-induced EM transition in A549 cells via Smad2 and Smad3, we evaluated the phosphorylation levels of these proteins. A549 cells were treated with IC261 for 4 h and then stimulated with TGF-β1 for 30 min. TGF-β1 treatment strongly induced the phosphorylation of Smad2 and Smad3 compared with that in the control group (Fig. 4). These effects were reversed when the cells were treated with IC261. We further analyzed downstream signaling pathways, such as the MAPKs (p38, ERK, JNK) and Akt signal pathways, and observed no significant change in the phosphorylation level (Additional file 2: Figure S2).

Effect of IC261 on TGF-β1-induced morphological changes in A549 cells

To analyze the effects of IC261 on TGF-β1-induced morphological changes of A549 cells, we observed the morphological and protein expression changes using confocal microscopy. A549 cells induced by TGF-β1 showed a mesenchymal phenotype, including cell papules and elongated spindle shapes. This mesenchymal phenotype induced by TGF-β1 was inhibited by IC261 pretreatment. Changes in protein expression were analyzed by immunofluorescence staining of Vim and N-cad. As shown in Fig. 5, the expression of Vim (upper panel) and N-cad (lower panel) was upregulated after TGF-β1 treatment. However, pretreatment with IC261 downregulated the expression of Vim and N-cad in a concentration-dependent manner in A549 cells (Fig. 5). These results are consistent with the immunoblot data shown in Fig. 2A. Therefore, IC261 inhibits TGF-β1-induced EM transition in A549 cells by altering the cellular morphology and EM transition transition-related protein expression.

IC261 inhibits TGF-β1-induced migration of A549 cells during EM transition transition

EM transition increases metastatic progression in various processes, as well as motility and resistance to invasiveness. A wound healing assay was performed to determine whether IC261 reduces TGF-β1-induced cell motility. TGF-β1 treatment enhanced cell mobility relative to that of control cells, whereas IC261 treatment significantly decreased this cell motility (Fig. 6A). Figure 6B shows the results of the wound healing assay, which indicate that IC261 prevents TGF-β1-stimulated migration of A549 cells.

Discussion

EM transition plays a vital role in cancer metastasis, including in migration and invasion, and is a critical step in cancer progression. TGF-β1 is a representative protein that induces EM transition, and the activation of TGF-β1 signaling pathways is essential for EM transition in vitro. TGF-β1-induced EM transition is mediated via the Smad2/3 signaling pathway. When cells are activated by TGF-β1, phosphorylated Smad2 and Smad3 form a complex with Smad4 and then translocate into the nucleus where they regulate the transcription of downstream EMT-related genes then, it governs cell proliferation, differentiation, and migration, including cellular homeostasis. As shown in Fig. 4, IC261 treatment inhibited TGF-β1-induced phosphorylation of Smad2 and Smad3 while did not affect the expression of total Smad2 and Smad3. Also, we recently reported that newly synthesized ent-caprolactin C (2) regulated EM transition by suppressing Smad 2/3 phosphorylation and then decreasing N-cad and β-cat in A549 cells [28, 29]. However, Smad-independent signaling can also induce EMT mediated by phosphatidylinositol 3 kinase–protein kinase B, mitogen-activated protein kinase, and MMPs [30]. In this study, we evaluated TGF-β1-induced cancer cell malignancy, focusing on the EM transition of A549 cells; this process is defined by the loss of cell–cell adhesion, transformation of the cell morphology, and acquisition of cellular motility. We examined whether IC261 inhibits TGF-β1-induced EM transition in A549 cells. IC261 suppressed TGF-β1-induced expression of N-cad, Vim, and β-cat protein and mRNA and prevented morphological changes. Furthermore, IC261 significantly inhibited TGF-β1-induced phosphorylation of Smad2 and Smad3, as well as significantly downregulated TGF-β1-stimulated migration of A549 cells in a concentration-dependent manner. Therefore, IC261 inhibited the initial steps of the TGF-β1 signaling pathway, such as Smad2 and Samd3 activation, to suppress EM transition in A549 cells (Fig. 7).

(See figure on next page.)

Fig. 6 Effects of IC261 on TGF-β1-induced migration in A549 cells. A549 cells were cultured as a monolayer in a 6-well plate (5.0×10^5 cells/well, plate); the cell cultures were replenished with serum-free culture medium after 24 h. The cells were treated with IC261 (50 and 75 μM) for 4 h, and then stimulated with TGF-β1 for 24 or 48 h. Time-lapse images of the scratch assay for each cell group were recorded at 0, 24, and 48 h using a digital camera (**A**). The relative wound width was calculated as the ratio of the width of the remaining wound at each time point to the corresponding width at 0 h using ImageJ software (**B**). Data are presented as the mean ± SD (n = 3). $^{\#}P < 0.0001$ compared with the controls, $^{***}P < 0.0001$ compared with the TGF-β1 group

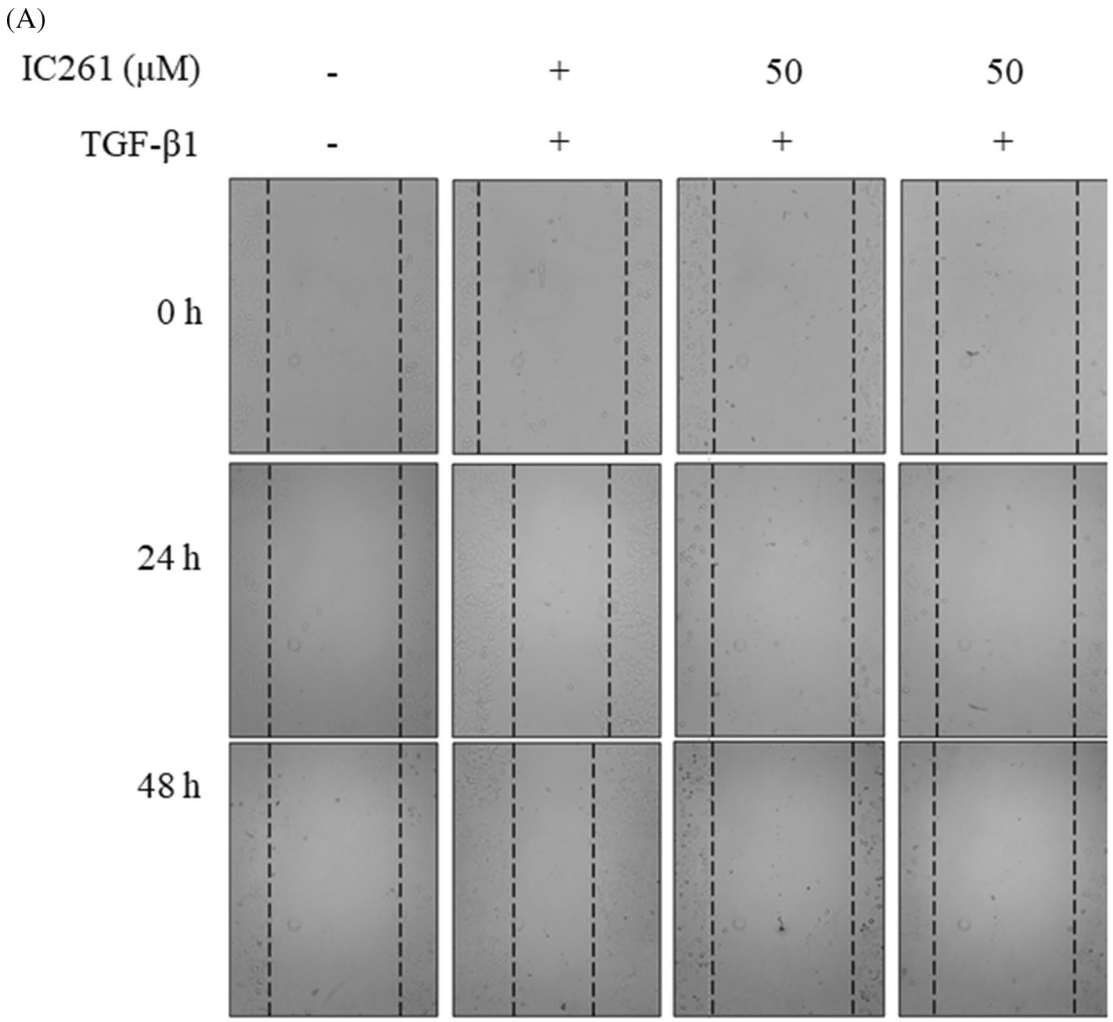

Fig. 6 (See legend on previous page.)

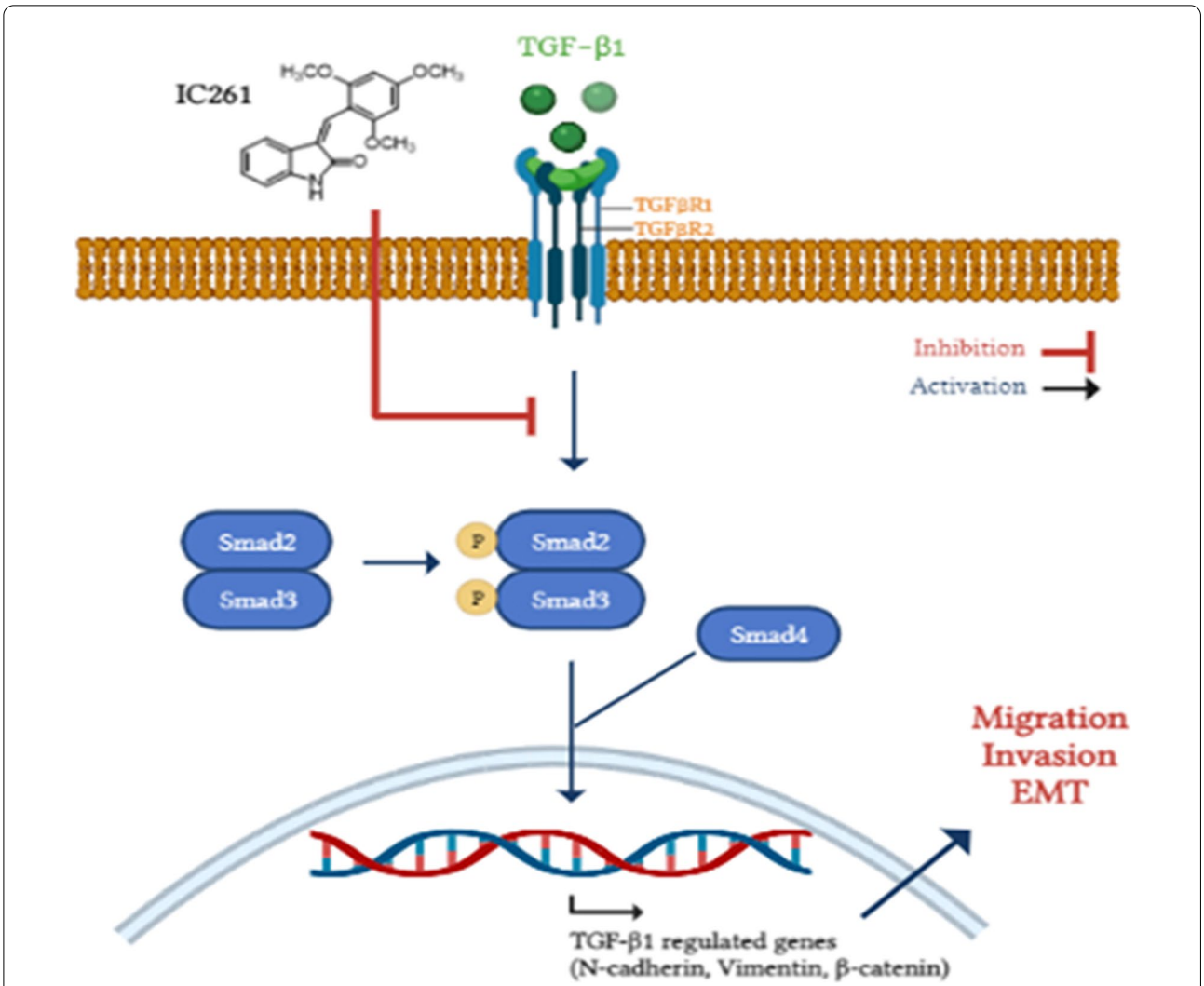

Fig. 7 Inhibitory mechanism of IC261 on TGF-β1-induced epithelial mesenchymal transition in A549 cells

IC261 is known to act as a multi-targeted anti-proliferative agent such as EGFR tyrosine kinase inhibition as well as hepatocellular carcinoma and colon cancer inhibitory effects [31, 32], and this study revealed that it has an EMT inhibitory effect. However, this study is limited to in vitro studies and requires further research on the anti-cancer effect of animal experiments. Also, Although the anti-cancer effects of these synthetic compounds are significant interest, promising preclinical studies are not generally translocated into clinical outcomes. Given the complex processes of initial target protein identification, optimization and the selectin of a candidate molecules for clinical development, further research in needed to elucidate the anti-cancer effects of IC261.

Abbreviations

β-cat: β-Catenin; CK: Casein kinase; DPBS: Dulbecco's phosphate buffered saline; EM transition: Epithelial mesenchymal transition; N-cad: N-cadherin; NSCLC: Non-small cell lung cancer; SCFM: Serum-free culture medium; TGF-β1: Transforming growth factor β1; Vim: Vimentin.

Supplementary Information

The online version contains supplementary material available at https://doi.org/10.1186/s13765-022-00690-1.

Additional file 1: Figure S1.

Additional file 2: Figure S2.

Acknowledgements

Not applicable.

Authors' contributions

SJ Kim and M-S Shin carried out the molecular genetic studies and drafted the manuscript. All authors read and approved the final manuscript.

Funding
This research was funded by a National Research Foundation of Korea (NRF) grant supported by the Korean government (MSIP), grant number NRF-2021R1F1A106378711.

Declarations

Competing interests
The authors declare that there is no conflict of interest.

Received: 18 January 2022 Accepted: 14 March 2022
Published online: 27 March 2022

References

1. Fares J, Fares MY, Khachfe HH, Salhab HA, Fares Y (2020) Molecular principles of metastasis: a hallmark of cancer revisited. Signal transduct Target Ther 5(1):1–17
2. Maurya DK, Nandakumar N, Devasagayam TPA (2010) Anticancer property of gallic acid in A549, a human lung adenocarcinoma cell line, and possible mechanisms. J Clin Biochem Nutr 48:85–90
3. Yao YH, Cui Y, Qiu XN, Zhang LZ, Zhang W, Li H, Yu JM (2016) Attenuated LKB1-SIK1 signaling promotes epithelial-mesenchymal transition and radioresistance of non-small cell lung cancer cells. Chin J Cancer 35:50
4. Ji M, Zhang Y, Shi B, Hou P (2011) Association of promoter methylation with histologic type and pleural indentation in non-small cell lung cancer (NSCLC). Diagn Pathol 6:48
5. Zhang T, Hu Y, Ju J, Hou L, Li Z, Xiao D, Li Y, Yao J, Wang C, Zhang Y, Zhang L (2016) Downregulation of miR-522 suppresses proliferation and metastasis of non-small cell lung cancer cells by directly targeting DENN/MADD domain containing 2D. Sci Rep 6:19346
6. Xu G, Yu H, Shi X, Sun L, Zhou Q, Zheng D, Shi H, Li N, Zhang X, Shao G (2014) Cisplatin sensitivity is enhanced in non-small cell lung cancer cells by regulating epithelial-mesenchymal transition through inhibition of eukaryotic translation initiation factor 5A2. BMC Pulm Med 14:174
7. Li L, Wu D (2016) mir-32 inhibits proliferation, epithelial–mesenchymal transition, and metastasis by targeting TWisT1 in non-small-cell lung cancer cells. Onco Targets Ther 9:1489–1498
8. Kin R, Kato S, Kaneto N, Sakurai H, Hayakawa Y, Li F, Tanaka K, Saiki I, Yokoyama S (2013) Procyanidin C1 from cinnamomi cortex inhibits TGF-β-induced epithelial-to-mesenchymal transition in the A549 lung cancer cell line. Int J Oncol 43:1901–1906
9. Lamouille S, Xu J, Derynck R (2014) Molecular mechanisms of epithelial–mesenchymal transition. Nat Rev Mol Cell Biol 15:178–196
10. Gugnoni M, Sancisi V, Gandolfi G, Manzotti G, Ragazzi M, Giordano D, Tamagnini I, Tigano M, Frasoldati A, Piana S, Ciarrocchi A (2017) Cadherin-6 promotes EM transition and cancer metastasis by restraining autophagy. Oncogene 36:667–677
11. Wang Y, Wen M, Kwon Y, Xu Y, Liu Y, Zhang P, He X, Wang Q, Huang Y, Jen KY, LaBarge MA, You L, Kogan SC, Gray JW, Mao JH, Wei G (2014) CUL4A induces epithelial-mesenchymal transition and promotes cancer metastasis by regulating ZEB1 expression. Cancer Res 74:520–531
12. Park GB, Kim D, Kim YS, Kim JW, Sun H, Roh KH, Yang JW, Hur DY (2015) Regulation of ADAM10 and ADAM17 by Sorafenib inhibits epithelial-to-mesenchymal transition in Epstein-Barr virus-infected retinal pigment epithelial cells. Invest Ophthalmol Vis Sci 56:5162–5173
13. Lamouille S, Xu J, Derynck R (2014) Molecular mechanisms of epithelial-mesenchymal transition. Nat Rev Mol Cell Biol 15:178–196
14. Suh SS, Yoo JY, Cui R, Kaur B, Huebner K, Lee TK, Aqeilan RI, Croce CM (2014) FHIT suppresses epithelial-mesenchymal transition and metastasis in lung cancer through modulation of microRNAs. PLoS Genet 10:e1004652
15. Cai G, Wu D, Wang Z, Xu Z, Wong K, Ng CF, Chan FL, Yu S (2017) Collapsin response mediator protein-1 (CRMP1) acts as an invasion and metastasis suppressor of prostate cancer via its suppression of epithelial-mesenchymal transition and remodeling of actin cytoskeleton organization. Oncogene 36:546–558
16. Tam WL, Weinberg RA (2013) The epigenetics of epithelial-mesenchymal plasticity in cancer. Nat Med 19:1438–1449
17. He K, Guo X, Liu Y, Li J, Hu Y, Wang D, Song J (2016) TUFM downregulation induces epithelial-mesenchymal transition and invasion in lung cancer cells via a mechanism involving AMPK-GSK3β signaling. Cell Mol Life Sci 73:2105–2121
18. Thiery JP, Acloque H, Huang RY, Nieto MA (2009) Epithelial-mesenchymal transitions in development and disease. Cell 139:871–890
19. Tomlinson DC, Baxter EW, Loadman PM, Hull MA, Knowles MA (2012) FGFR1-induced epithelial to mesenchymal transition through MAPK/PLCγ/COX-2-mediated mechanisms. PLoS ONE 7:e38972
20. Ko H (2015) Geraniin inhibits TGF-β1-induced epithelial–mesenchymal transition and suppresses A549 lung cancer migration, invasion and anoikis resistance. Bioorg Med Chem Lett 25:3529–3534
21. Ko H, Jeon H, Lee D, Choi HK, Kang KS, Choi KC (2015) Sanguiin H6 suppresses TGF-β induction of the epithelial-mesenchymal transition and inhibits migration and invasion in A549 lung cancer. Bioorg Med Chem Lett 25:5508–5513
22. Behrend L, Milne DM, Stöter M, Deppert W, Campbell LE, Meek DW, Knippschild U (2000) IC261, a specific inhibitor of the protein kinases casein kinase 1-delta and-epsilon, triggers the mitotic checkpoint and induces p53-dependent postmitotic effects. Oncogene 19:5303–5313
23. Brockschmidt C, Hirner H, Huber N, Eismann T, Hillenbrand A, Giamas G, Radunsky B, Ammerpohl O, Bohm B, Henne-Bruns D, Kalthoff H, Leithäuser F, Trauzold A, Knippschild U (2008) Anti-apoptotic and growth-stimulatory functions of CK1 delta and epsilon in ductal adenocarcinoma of the pancreas are inhibited by IC261 in vitro and in vivo. Gut 57:799–806
24. Liu M, Hu Y, Lu S, Lu M, Li J, Chang H, Jia H, Zhou M, Ren F, Zhong J (2020) IC261, a specific inhibitor of CK1δ/ε, promotes aerobic glycolysis through p53-dependent mechanisms in colon cancer. Int J Biol Sci 16:882–892
25. Smith AL, Robin TP, Ford HL (2012) Molecular pathways: targeting the TGF-β pathway for cancer therapy. Clin Cancer Res 18:4514–4521
26. Grünert S, Jechlinger M, Beug H (2003) Diverse cellular and molecular mechanisms contribute to epithelial plasticity and metastasis. Nat Rev Mol Cell Biol 4:657–665
27. Jeong JH, Jang HJ, Kwak S, Sung GJ, Park SH, Song JH, Kim H, Na Y, Choi KC (2019) Novel TGF-β1 inhibitor antagonizes TGF-β1-induced epithelial-mesenchymal transition in human A549 lung cancer cells. J Cell Biochem 120:977–987
28. Kim SY, Shin MS, Kim GJ, Kwon H, Lee MJ, Han AR, Nam JW, Jung CH, Kang KS, Choi H (2021) Inhibition of A549 lung cancer cell migration and invasion by *ent*-caprolactin C via the suppression of transforming growth factor-β-induced epithelial-mesenchymal transition. Mar Drugs 19:465
29. Lee MJ, Kim GJ, Shin MS, Moon J, Kim S, Nam JW, Kang KS, Choi H (2021) Chemical investigation of diketopiperazines and N-phenethylacetamide isolated from *Aquimarina* sp. MC085 and their effect on TGF-β-Induced epithelial-mesenchymal transition. Appl Sci 11(19):8866
30. Luo Y, Ren Z, Du B, Xing S, Huang S, Li Y, Lei Z, Li D, Chen H, Huang Y, Wei G (2019) Structure identification of viceninII extracted from Dendrobium officinale and the reversal of TGF-β1-induced epithelial–mesenchymal transition in lung adenocarcinoma cells through TGF-β/Smad and PI3K/Akt/mTOR signaling pathways. Molecules 24:144
31. Fareed MR, Shoman ME, Hamed MI, Badr M, Bogari HA, Elhady SS, Ali TF (2021) New multi-targeted antiproliferative agents: Design and synthesis of IC261-based oxindoles as potential tubulin, CK1 and EGFR Inhibitors. Pharmaceuticals 14(11):1114
32. Yuan F, Li D, Guo M, Fang T, Sun J, Qi F, Xia J (2020) IC261 suppresses progression of hepatocellular carcinoma in a casein kinase 1 δ/ε independent manner. Biochem Biophys Res Commun 523(3):809–815

Publisher's Note